

2D and 3D impellers of centrifugal compressors – advantages, shortcomings and fields of application

Y Galerkin, A Reksrin, A Drozdov

R&D Laboratory “Gas dynamics of turbo machines” Peter the Great St. Petersburg Polytechnic University, Polytechnical st. 29, St.Petersburg, Russia

Email: buck02@list.ru.

Abstract: The simplified equations are presented for calculation of inlet dimensions and velocity values for impellers with three-dimensional blades located in axial and radial part of an impeller (3D impeller) and with two-dimensional blades in radial part (2D). Considerations concerning loss coefficients of 3D and 2D impellers at different design flow rate coefficients are given. The tendency of reduction of potential advantages of 3D impellers at medium and small design flow rate coefficients is shown. The data on high-efficiency compressors and stages with 2D impellers coefficients designed by the authors are presented. The reached efficiency level of 88 - 90% makes further increase of efficiency by the application of 3D impellers doubtful. CFD-analysis of stage candidates with medium flow rate coefficient with 3D and 2D impellers revealed specific problems. In some cases the constructive advantage of a 2D impeller is smaller hub ratio. It makes possible the reaching of higher efficiency. From other side, there is a positive tendency of gas turbine drive RPM increase. 3D impellers have no alternative for stages with high flow rate coefficients matching high-speed drive.

Nomenclature

b	width of channel
c	absolute velocity at an impeller exit
D	diameter
K_D	geometry parameter of 2D impeller
K_F	geometry parameter of 2D impeller
l	length
L_m	impeller meridian length
M	Mach number
\bar{m}	mass flow rate
u	blade velocity
w	relative velocity
α	flow angle related to tangent
β_{bl}	blade angle related to tangent
χ	angle between blade and meridian surfaces
ρ	gas density
ζ	loss coefficient
τ	blade blockage factor



ψ_T	loading factor
φ	flow coefficient
η	efficiency
π	pressure ratio
Φ	flow rate coefficient

Subscripts

1	impeller inlet
2	impeller exit
h	hub
des	design flow rate
m	meridian
min	minimum
max	maximum
s	shroud
inl	inlet

1. Main features of 2D and 3D impellers

Radial impellers with blades of a cylindrical form are used in industrial centrifugal compressors since the end of 19th century. Fig. 1 demonstrates 2D impeller with stamped blades riveted to impeller discs. These were widely applied in the past. Late decision is a 2D impeller with milled blades on the surface of the main disk. Process of blade milling is shown in Fig. 1.

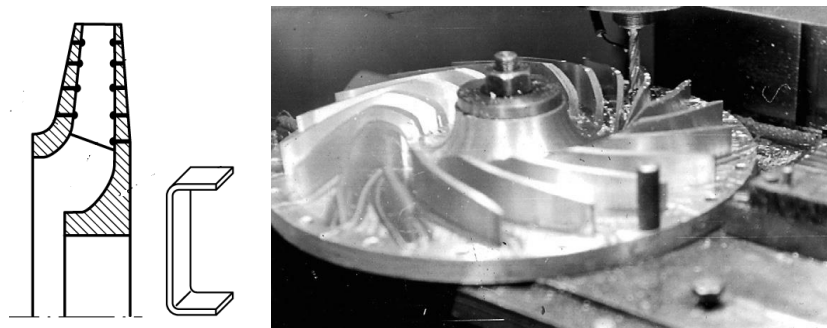


Figure 1. Classical impeller with stamped and riveted blades and element of a stamped blade – left. Milling of blades with cylindrical surface – photo on the right [1]

Manufacturing technology of 2D impellers is convenient for individual and small-scale production. In general, in pipeline and industrial compressors 2D impellers are widely applied. However, from the aerodynamic point of view, the cylindrical shape of blades contradicts the three-dimensional character of a flow. Especially this contradiction seems important at an impeller inlet. Inlet flow angle varies in a wide range along blade leading edge. The design technique applied by authors [1], allows to solve this problem for 2D impellers with limited design flow rate coefficients.

The impellers with 3D blades and leading edges in an axial part were applied firstly in aviation gas-turbine engines. Their obvious advantage is the highest durability at high blade velocity. 3D impellers are more effective at high Mach number and big loading factor.

Five-coordinate milling machines with numerical control made possible application of 3D impellers in industrial compressors. Fig. 2 shows 3D impeller for an industrial compressor. A meridional configuration of 3D and 2D impellers is presented in Fig. 3.



Figure 2. 3D impeller, closed type – left, blade cascade - right

Pipeline compressors operate at low blade velocity and low Mach numbers. They have low loading factors in most cases. Advantages of 3D impellers for pipeline compressors are not evident if flow rate coefficients are not too high. The efficiency of 3D and 2D impeller is analyzed below.

The loss of efficiency in the impeller depends on dimensionless relative velocity at an inlet taking into account blade blockage factor [1]:

$$\Delta\eta_{\text{imp}} = \zeta_{\text{imp}} \frac{\bar{w}'_1{}^2}{2\psi_{T\text{des}}} \quad (1)$$

Here \bar{w}'_1 is an average velocity along a blade leading edge.

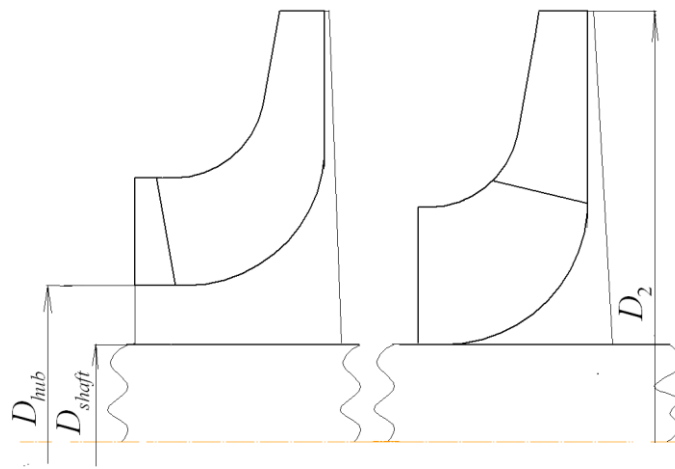


Figure 3. Impellers' meridian schemes. 3D – left, 2D – right

To minimize efficiency loss it is necessary to minimize \bar{w}'_1 . The loss coefficient minimization depends on a design skill and impeller relative dimensions.

2. Inlet and outlet dimensions and flow velocities

If a leading edge of a 3D impeller is placed as shown in Fig. 3:

$$\bar{w}'_0 = \sqrt{\bar{D}_0^2 + \phi_0'^2} \quad (2)$$

For 2D impeller:

$$\bar{w}'_1 = \sqrt{\bar{D}_1^2 + \phi_1'^2} \quad (2a)$$

Relative inlet diameter and flow rate coefficient are connected by the continuity equation.

For 3D impeller:

$$\bar{m} = \rho_0^* \cdot \Phi_{des} u_2 \frac{\pi}{4} D_2^2 = \rho'_0 \cdot \varphi'_0 u_2 \cdot \tau_0 \frac{\pi}{4} (D_0^2 - D_{hb}^2) = \rho'_0 \cdot \varphi'_0 u_2 \cdot \tau_0 \frac{\pi}{4} 2b_0 (D_0 + D_{hb}), \text{ and:}$$

$$\varphi'_0 = \frac{\rho_0^*}{\rho'_0} \frac{\Phi_{des}}{\tau_0 (\bar{D}_0^2 - \bar{D}_{hb}^2)} = \frac{\rho_0^*}{\rho'_0} \frac{\Phi_{des}}{\tau_0 2\bar{b}_1 (\bar{D}_0 + \bar{D}_{hb})} \quad (3)$$

For 2D impeller $\bar{m} = \rho_0^* \cdot \Phi_{des} \frac{\pi}{4} D_2^2 u_2 = \rho'_1 \cdot \varphi'_1 \cdot \tau_1 \pi D_1 b_1 u_2$, and:

$$\varphi'_1 = \frac{\rho_0^*}{\rho'_1} \frac{\Phi_{des}}{4\tau_1 \bar{D}_1 \bar{b}_1} \quad (3a)$$

Here Φ_{des} - flow rate coefficient, which connects mass flow rate with an impeller diameter and blade velocity [1]:

$$\Phi_{des} = \frac{\bar{m}_{des} / \rho_0^*}{\pi \frac{D_2^2}{4} u_2} \quad (4)$$

The designer can choose the necessary design flow rate coefficient if RPM or number of stages are not constrained [1]. It is not so for most pipeline compressors.

According to the equations (2, 2a) to a bigger inlet diameter corresponds a smaller flow rate coefficient but bigger blade velocity $\bar{u}_1 = \bar{D}_1$. Minimal inlet velocities can be calculated by the

formulae [1]. For 3D: $\bar{D}_{0w\min} = \sqrt{\bar{D}_{hb}^2 + 2^{\frac{1}{3}} \left(\frac{\Phi_{des}}{\frac{\rho'_0}{\rho_0^*} \tau_0} \right)^{\frac{2}{3}}}$. For 2D: $\bar{D}_{1w\min} = K_D \sqrt{\bar{D}_{hb}^2 + 2^{\frac{1}{3}} \left(\frac{\Phi_{des} K_F}{\frac{\rho'_1}{\rho_0^*} \tau_1 K_D} \right)^{\frac{2}{3}}}$, for

the approximate analysis we will accept typical values of parameters of a secondary importance:

- ratio of static and total parameter density $\frac{\rho'_1}{\rho_0^*}$ is 0,9,
- blade blockage factor τ_1 is 0,85,
- geometry coefficient K_D [1] is 1,0,
- geometry coefficient K_F [1] is 0,85.
- inlet blade blockade factor τ_1 [1] is 0,85.

Then:

$$\bar{D}_{0w\min} \approx \left(\bar{D}_{hb}^2 + 1,5\Phi_{des}^{2/3} \right)^{0,5}, \quad (5)$$

$$\bar{D}_{1wmin} \approx \left(\bar{D}_{hb}^2 + 1,35\Phi_{des}^{2/3} \right)^{0,5}. \quad (5a)$$

In Fig. 3 above is shown that a shaft diameter can be equal to diameter of the hub of a 2D impeller. A hub of a 3D impeller sometimes is bigger. A shaft diameter must provide the necessary rigidity of a rotor. Bigger diameter of the hub doesn't increase rigidity, but worsens 3D impeller gas dynamic properties.

A flow coefficient in eq. (2), (2a) depends on an inlet blade height. From a geometrical ratio $D_0 - D_{hb} = 2b_0$:

$$\bar{b}_0 = \frac{\left(\bar{D}_{hb}^2 + 1,5\Phi_{des}^{2/3} \right)^{0,5} - \bar{D}_{hb}}{2}. \quad (6)$$

From a geometrical ratio $\left((D_1 / K_D)^2 - D_{hb}^2 \right) = K_F 4D_1 b_1$:

$$\bar{b}_1 = 0,4 \frac{\Phi_{des}^{2/3}}{\left(\bar{D}_{hb}^2 + 1,35\Phi_{des}^{2/3} \right)^{0,5}} \quad (6a)$$

From equations (5) and (3):

$$\varphi'_0 \approx 0,70\Phi_{des}^{1/3} \quad (7)$$

From equations (5a) and (3a):

$$\varphi'_1 \approx 0,82\Phi_{des}^{1/3}. \quad (7a)$$

Non- dimensional inlet velocity on a diameter D_0 of a 3D impeller:

$$\bar{w}'_0 \approx \sqrt{\bar{D}_{hb}^2 + 2\Phi_{des}^{2/3}}. \quad (8)$$

Non-dimension inlet velocity in 2D impeller:

$$\bar{w}'_1 \approx \sqrt{\bar{D}_{hb}^2 + 2\Phi_{des}^{2/3}} \quad (8a)$$

Equal values of velocities \bar{w}'_0 and \bar{w}'_1 in equations (8) and (8a) is a coincidence at the accepted typical values $K_D=1,0$, $K_F=0,85$: $\frac{\rho_0^*}{\rho_0'}=0,9$ and $\tau_0 = \tau_1=0,85$. But at the same time it is a demonstration of the fact that velocities \bar{w}'_0 and \bar{w}'_1 are close in principle. The next considerations must be taken into account:

- a leading edge of 3D impeller blades is located between the hub and shroud discs. Dimensionless relative velocity is maximal at a shroud and minimal at a hub due to change of

a leading edge velocity. An average value of \bar{w}'_0 is less than practically constant value of \bar{w}'_1 . 3D impellers have an advantage;

- hub ratio of 2D impeller can be smaller. Then $\bar{w}'_1 < \bar{w}'_0$ in accordance with equations (8) and (8a). 2D impellers have advantage.

3. Loss coefficients of 3D and 2D impellers. General assessment of application

The obvious opportunity to minimize profile losses due to 3D profiling induces some producers to apply this technology in all range of design flow rate coefficients. The 3D impeller family presented in paper [2].

Calculation analysis shows that at $\Phi_{des} < 0,05-0,06$ disc friction losses prevail on profile losses [3].

Loss coefficient of 3D impellers $\zeta_{3D} = 0,5 \frac{\bar{w}'_0^2}{\Psi_T}$ are more than 0.19 while loss coefficient of 2D impellers are usually less than 0.14. Here are meant impellers with $\Phi_{des} = 0,05-0,07$, designed by the technique used by authors [1, 3]).

4. Examples of high-efficiency compressors and stages with 2D impellers

In [4-6] there is an information on factory tests or model tests of compressors designed by the team of Prof. Y. Galerkin, including other authors of the paper. In total more than 400 of designed compressors are constructed with a total power that exceeds 5 million kW. The performances of the four-stage pipeline compressor and results of their modeling by the 5th version of Universal modeling method are shown in Fig. 4. The maximum efficiency of the compressor is 0.875. The maximum efficiency of its 1st stage is 0.888. The stage design flow rate coefficient is $\Phi_{des} = 0,0633$, the design loading factor $\Psi_{T des} = 0.42$.

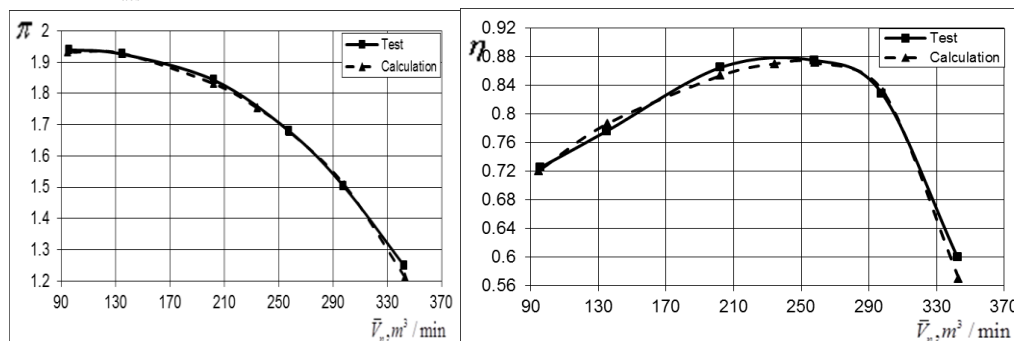


Figure 4 Gas dynamic performances of the four-stage pipeline compressor. Factory test and modeling calculation [4]

For 32 MW pipeline compressors the industrial partner offered high-speed drive with 5500 RPM and effective single-stage scheme. An axial inlet application, vaneless diffuser with optimal dimensions and design optimization procedure has led to high-efficiency solution that was proven by model tests, in scale 1:2. The model cross section, design and test performances are presented in Fig. 5.

Efficiency and polytrophic head coefficient performances are predicted with good accuracy by the Universal Modeling Method [7, 8]. The maximum efficiency equals 90%, is confirmed experimentally. 2D blade height on an inlet is equal to 0,11. The non-incidence flow at inlet along a leading edge is achieved anyway.

The examples support the authors' opinion that 3D impeller application hardly could rise pipeline and alike other industrial compressors efficiency if design flow rate coefficient of stages does not exceed 0,070 – 0,075.

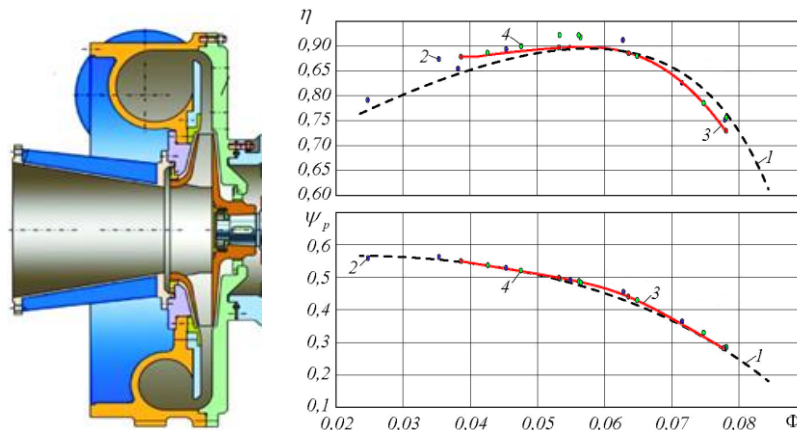


Figure 5. The model of the 32 MW pipeline compressor, in scale 1:2 (left). Test results and calculations (right) 1- design performance, 2- $M_u = 0.705$, 3- $M_u = 0.710$, 4- $M_u = 0.700$ [9]

5. Numerical analysis of candidate stages with 3D and 2D impellers

The stage with design parameters $\Phi_{des} = 0,068$, $\psi_{T_{des}} = 0,50$ was chosen for efficiency comparison. Stator elements are a vaneless diffuser and a return channel.

The initial 3D candidate impeller was designed in accordance with recommendations proven for high flow rate 3D impellers [3].

Non-viscid Q3D approach is used for velocity calculation. The principles of Q3D non-viscid calculation and design procedure of an impeller on the basis of this approach are described in [1]. Some of design recommendations based on general principles and on high flow rate impeller numerical study [3]:

- inlet diameter D_0 is about 0.91 of a diameter calculated by the formula (5),
- a leading edge is located at a distance 0.25 of a meridian length from an inlet section "0",
- blade 3D configuration is based on velocity diagram analysis and optimization,
- an exit blade angle β_{bl2} is increased from hub to shroud,
- a blade surface generatrix at an impeller exit χ_2 is inclined to a direction of rotation to diminish blade surface area.

These principles were applied to the candidate #1 design. Information on this and other candidates is presented in the Table 1.

Symbol $\beta_{bl2}(b_2) = \text{var}$ means that its value at a shroud is bigger than at a hub. If a blade surface generatrix at an impeller exit χ_2 is inclined to a direction of rotation then $\chi_2 < 0$.

The NUMECA Fine Turbo program was applied for calculations. The grid consists of 1,8 million cells. The Spallart-Almaras model of turbulence was used. Boundary conditions:

- on an inlet: total pressure and total temperature;
- at the outlet: mass flow rate.

Friction of external surfaces of impeller discs and labyrinth seal leakage weren't modelled.

Table 1. Candidate impellers' main parameters 2D and 3D

Candidates	Type	\bar{D}_{hub}	\bar{L}_m	$\bar{c}_m(b)$	$\beta_{bl2}(b_2)$	χ_2	$\eta_{max} \%$
1	3D	0,363	0,22	no unif.	var	-10	84,5
2	3D	0,363	0,28	no unif.	var	-10	84,5
3	3D	0,363	0,25	unif.	const	30	86,1
4	2D	0,363	-	unif.	const	0	86,2
5	2D	0,325	-	unif.	const	0	88,5
2D analog	2D	0,24	-	unif.	const	0	88,5 calc/87,9 test

Calculations overestimate a design loading factor by 6–12%. Calculated performances are shifted to bigger flow rate. But measured and calculated maximum efficiency coincides. The candidate stages are compared on the maximum efficiency therefore. Their efficiency performances are presented in Fig. 6. Candidates' numbers are the same as in table 1.

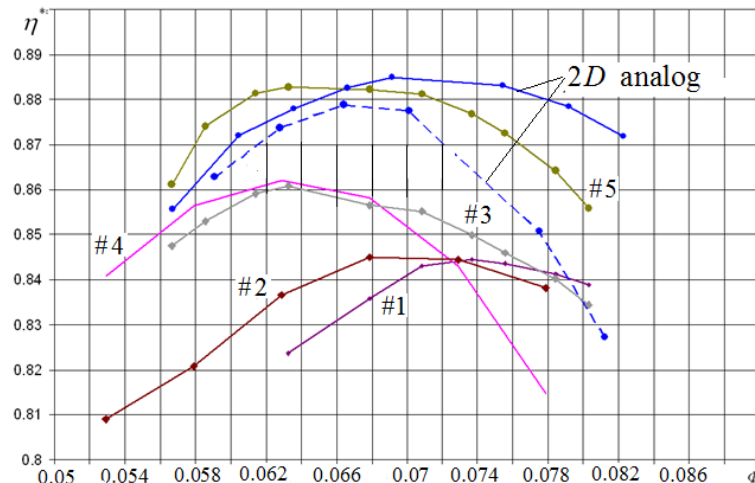


Figure 6. Efficiency performance curves of candidate stages and of 2D analog (stroke line – measurement)

There is information on the stage “2D analog” in the table 1. It is one of stages with 2D impeller from the database of the Laboratory of gas dynamics of turbomachines. Measured and calculated efficiency performances are presented in Fig. 6. The calculated performance is overestimate efficiency at high flow rates as in other cases. Parasitic losses were not taken into account at CFD-calculation. Meaning it, the CFD-calculation predicts maximum efficiency of a stage well enough.

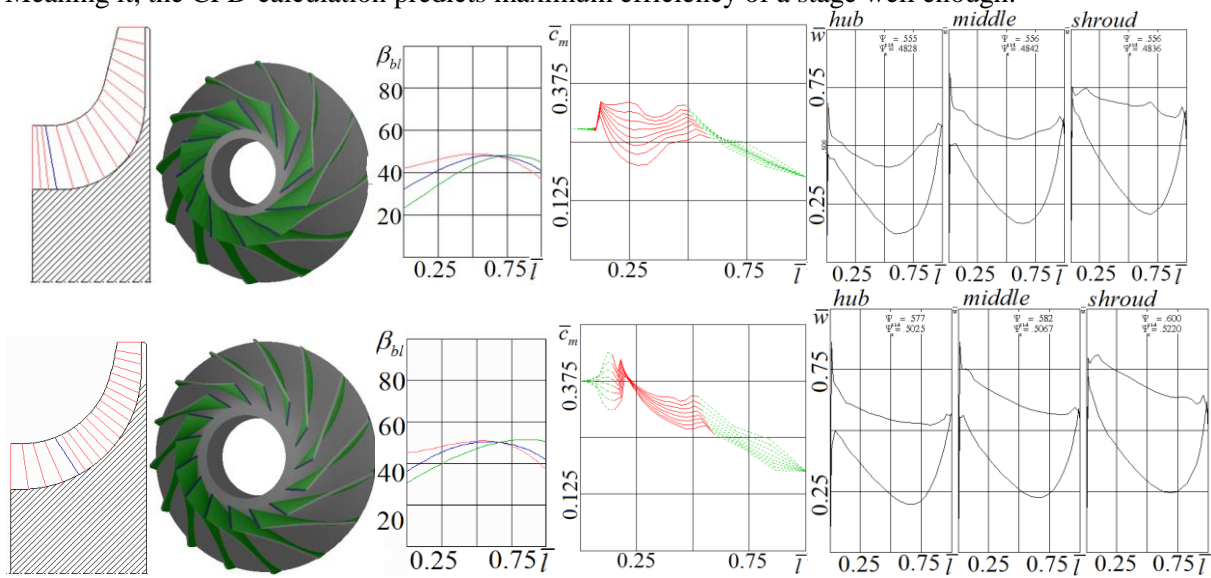


Figure 7. 3D Impeller candidate #1(above) and #2 (below). From left to right: meridian configuration, blade cascade view, blade angles on three blade to blade surfaces along meridian coordinate, meridional velocities on eight blade-to-blade surfaces, blade velocity diagrams on hub, mean, shroud blade to blade surfaces

The candidate #1 was designed by the principles that are mentioned above. The information on this candidate is presented in fig. 7.

The design flow rate coefficient of the candidate #1 and others is by 35% less than that of the analog in Fig. 6. Hub relative diameter is by 32% bigger. The meridional contour is made with a reduced axial dimension.

The maximum efficiency of the candidate #1 is 84.5%. Angles of absolute velocity at an impeller exit along a trailing edge $\alpha_2 = f(b/b_2)$ are shown in Fig. 8. One of the reasons of the stage low efficiency and poor performance left from a design point is negative flow angle near a shroud already at the design flow rate. It provokes flow separation in a vaneless diffuser.

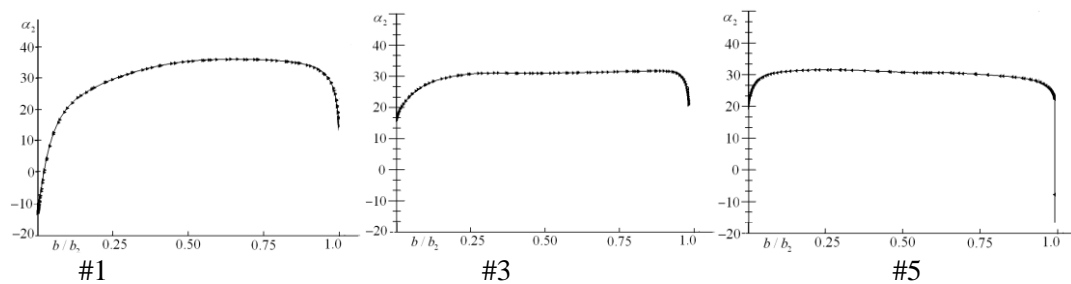


Figure 8. Absolute velocity angles along trailing for candidates ## 1, 3, 5. Design flow rate. Shroud is at the left

The candidate #2 was designed by the same principles, as #1, but its meridional dimension is bigger and is closer to the analog with $\Phi_{des} = 0.105$. Fig. 7 provides information on the candidate #2. The exit flow angle diagram $\alpha_2 = f(b/b_2)$ in Fig. 8 is much better. The maximum efficiency is on the same level but the stage operates much better than the candidate #1 (Fig. 6).

The candidate #3 has a 2D impeller – Fig. 9. The maximum efficiency of the stage is by 1.5% higher than that of the candidates ##1 and 2 with 3D impellers. The diagram $\alpha_2 = f(b/b_2)$ in Fig. 10 demonstrates the best uniformity.

Velocity diagram comparison has pointed on different characters of meridian velocity diagrams in 3D and 2D impellers. In 2D impellers meridian flow non uniformity is high near a leading edge. The meridian velocities become uniform in the second part of a blade channel. Meridian velocities are sufficiently non uniform in all 3D blade channels. Diagrams $\bar{c}_m = f(l_{mi}/l_m)$ in Fig. 7 demonstrates it. Symbol “non uniform” points on the fact in the table 1.

The candidate #3 was designed meaning the goal to reach maximum possible for 3D impeller uniformity (symbol “unif.” in table 1) of $\bar{c}_m = f(l_{mi}/l_m)$ diagram. The candidate has a positive angle $\chi_2 = +30^\circ$ and constant blade exit angle along a trailing edge. Information on the candidate #3 is presented in Fig. 9.

Meridian velocity diagram is not alike diagrams of 2D impellers. But it is the most uniform for 3D impeller of given parameters. The positive result is obvious. The maximum efficiency of the candidate #3 is the highest among 3D and is equal to efficiency of the candidate #4 with 2D impeller.

The candidate #5 realizes the constructive advantage of 2D impellers. Its non dimensional hub ratio is 0.325 against 0.363 of the candidates with 3D impellers. The principle of design is the same as for the candidate #4. The efficiency of this candidate is 88,2%. Advantage of the candidate #5 on efficiency is 2.1%. It is a result of not only lower kinetic energy of a flow at an inlet. The minimum loss coefficient of the candidate impeller #5 is 0,132 against 0,173 of the candidate #4. The authors can not explain this result of CFD calculation, as design principles and all parameters of the impellers #4 and #5 are similar.

CFD – calculations have provided extensive information on structure of a flow in the candidates. Samples of velocity fields are shown in Fig. 10 for the candidates ##1, 3 and 5. Fields of velocities are

presented on two blade to blade surfaces– near the shroud and near the hub (design flow rate). Low-energy zones of various intensity take place in all three candidates: #1 – the lowest efficiency, #3 – the best of 3D, #5 – the best of all. It is remarkable that in the 2D impeller a favorable character of flow is identical on surfaces near a shroud and a hub. Visual impression is that the 2D candidate has identical blade cascades in near the shroud and the hub. On the contrary, blade cascades of 3D candidates seem too dense near a hub.

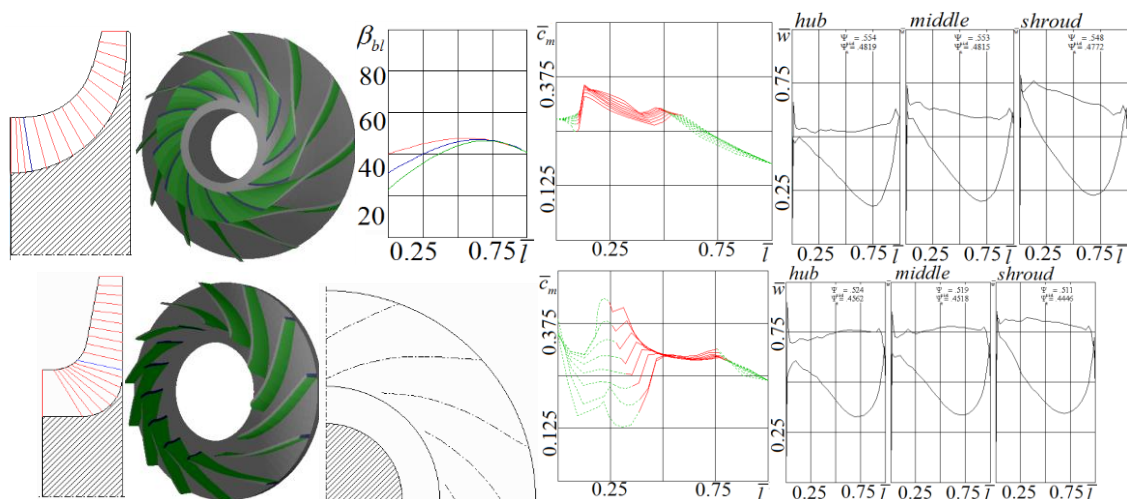


Figure 9. 2D impeller candidate #3 (above) and #4 (below). From left to right: meridian configuration, blade cascade view, blade angles on three blade to blade surfaces along meridian coordinate, meridional velocities, blade velocity diagrams on blade to blade surfaces

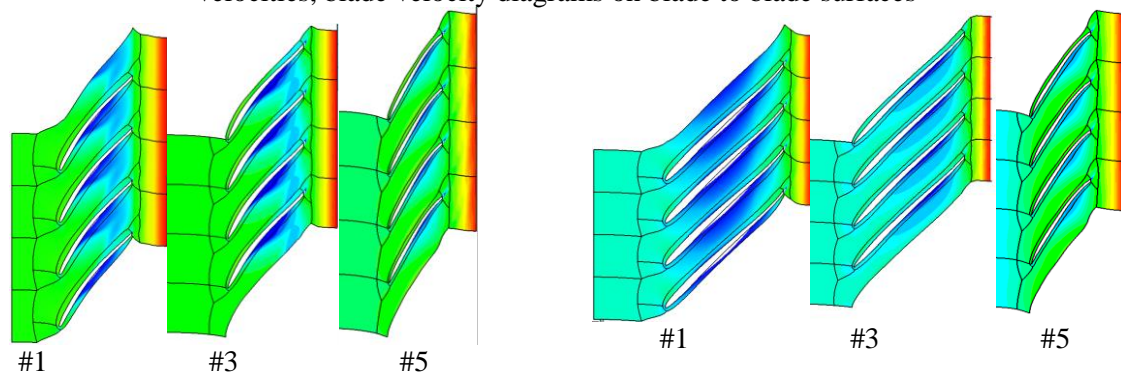


Figure 10. Flow fields on two blade to blade surfaces. Design flow rate. 10% from shroud – left, 10% from hub - right

Conclusion

The authors are sure that at low Mach number and medium and low loading factor 2D impellers are better if a design flow rate $\Phi_{des} < 0.07-0.08$. Compressor users insist on 3D impellers application in areas where they sometimes have no advantages. Properly designed compressor with 2D impellers can be cheaper and not less effective in many cases.

From the other side there are no doubts that the advantages of high flow rate stages with $\Phi_{des} \geq 0.07-0.08$ can be achieved only by application of 3D impellers. High flow rate stages effective design principles deserve proper attention.

Acknowledgment

The reported study was funded by RFBR according to the research project № 16-08-00624 A.

References

- [1] Galerkin Y. Turbo compressors. [text] / Gale2Din, Y. // LTD information and publishing center. - Moscow. – KHT. - 2010. - P. 596. [Russian].
- [2] Higauti, X. Development and use of gas injection compressor ultra-high pressure of 700 bar. / Transactions of the 19 international symposium «COMPRESSOR users-manufacturers – 2015». – SPb. – SPbTU. – 2015. – P. 12-21. [Russian].
- [3] Galerkin Y., Drozdov A. Modeling of gas dynamic characteristics of centrifugal compressor stages with 3D impellers. Scientific and technical transactions of the TU SPb. - SPb. -2014. - № 3(202). - P. 45-53. [Russian].
- [4] Galerkin Y., Soldatova K. Operational process modeling of industrial centrifugal compressors. Scientific bases, development stages, current state. Monograph. SPb – 2011. – P. 327. [Russian].
- [5] Galerkin, Y.B., Soldatova, K.V. Working out of «virtual» modeling stages by means of programs of the 5th generation of the method of universal modeling. Scientific and technical transactions of the TU SPb. – 2011. – No. 4. – Page 241-248. [Russian].
- [6] Soldatova K. Universal modeling method loss and wo2D input models verification on results of industrial compressors test. Scientific and technical transactions of the TU SPb. - 2010. – No. 4. – P. 300-308. [Russian].
- [7] Galerkin, Y. B., Soldatova, K.V. Universal modeling method application for development of centrifugal compressor model stages. International Conference on Compressors and their systems. – London: City University. – UK. – 2013. – P. 477-487.
- [8] Galerkin Y., Soldatova K., Drozdov A. Modern state of the universal modeling for centrifugal compressors. International Conference on Numerical Methods in Industrial Processes. World Academy of science, engineering and technology. Paris 2015 Conference. <http://www.waset.org/Publications/?path=Publications>. - Vol:9 No:01 2015. – № 242.
- [9] A.V. Smirnov, V.G. Panenko, V.G. Gadiaka, V.P. Parafeynik, A.M. Borodenko (Sumy Frunze NPO PJSC). High Efficiency Centrifugal Compressor New Design for the GPA-C32/76-1.35 Compressor Package Applied at Gas Main Compressor Stations. // Compressors and pneumatics. - 2015. – № 3. – P. 12-16. [Russian].